J Inorg Organomet Polym (2015) 25:107–117
DOI 10.1007/s10904-014-0108-y

Synthesis and Photovoltaic Properties of 2D π-Conjugated Polymers Based on Alkylbenzothiophene Substituted Benzodithiophene Donor Unit with Titanium Sub-Oxide (TiO_X) as an Interlayer in the Bulk Heterojunction Device Structure

Nallan Chakravarthi · Kumarasamy Gunasekar · Sung-Ho Jin · Jun Hee Lee

Received: 14 August 2014 / Accepted: 6 October 2014 / Published online: 15 October 2014

Abstract A newbenzo[1,2-b:4,5-b']dithiophene (BDT) derivative with conjugated side chain substituent, 5-ethylhexylbenzothiophene group, was synthesized as donor unit (D) and copolymerized with two acceptor units (A), 3,3′-diethylhexyl-3,4-propylenedioxythienyl-bisbenzothiadiazole and 3,6-di(thiophen-2-yl)pyrrolo[3,4-c]pyrrole-1,4(2H,5H)-dione (DPP), respectively, using Stille coupling reaction to afford two new copolymers, **P1** and **P2**. Low bandgaps were successfully accomplished for P1 (1.64 eV) and P2 (1.37 eV) and were attributed to the strong intramolecular charge transfer within the D–A alternating structure. Both **P1** and **P2** exhibited highest occupied molecular orbital (HOMO) energy levels that were deeper due to the conjugated benzothiophene substituent. The photovoltaic performances of the synthesized polymers were investigated using the device configuration ITO/PEDOT:PSS/polymer:$PC_{71}BM$/(with or without)TiO_x/Al. We employed titanium sub-oxide (TiO_x) as an effective interlayer in the bulk heterojunction device structure. The subsequent photovoltaic performances showed high open-circuitvoltages (V_{oc}) ranging from 0.78 to 0.81 V, whereas the power conversion efficiencies (PCEs) depended strongly on the blend morphologies. The polymer solar cell devices based on the blend of **P2** and $PC_{71}BM$ gave the best photovoltaic performance among the series, with a V_{oc} of 0.78 V, short-circuit current density (J_{sc}) of 5.69 mA/cm^2, fill factor (FF) of 58.09 % and PCE of 2.60 %.

Keywords Benzothiophene Bandgap Titanium sub-oxide Power conversion efficiency

1 Introduction

Benzodithiophene (BDT) based semiconducting π-conjugated polymers have acquired much interest in the past two decades due to their ultimate performances in polymer solar cells (PSCs) as well as organic field effect transistors (FETs) [1]. The BDT core provides the flexibility of attaching different conjugated side chain substituents on the central phenyl core to modulate the frontier orbital energy levels of the polymers along with its highly planar backbone structure [2]. Several conjugated side chain substituents such as alkyl, alkoxy, alkylthienyl, and phenyl have been introduced by various research groups to the central benzene ring of BDT [3–8]. Our group independently reported the synthesis and electronic properties of BDT based polymers with alkylselenyl substituents [9].BDT unit display strong π–π stacking and good hole mobilities due to their high planarity and small steric hindrance between adjacent molecules. For the past 2 years, 5-alkylthiophene-2-yl-substituted BDT (BDTT) unit have been thriving as electron donor unit for synthesizing highly efficient polymeric entities [10]. The 2D copolymers based on BDTT showed better thermal stabilities, highest occupied molecular orbital (HOMO) and

Article Note N. Chakravarthi and K. Gunasekar have contributed equally to this manuscript.

N. Chakravarthi · K. Gunasekar · S.-H. Jin (✉)
Department of Chemistry Education, Graduate Department of Chemical Materials, BK 21 PLUSTeam for Advanced Chemical Materials, and Institute for Plastic Information and Energy Materials, Pusan National University, Busan 609-735, Republic of Korea
e-mail: shjin@pusan.ac.kr

J. H. Lee
Department of Advanced Materials Engineering, Dong-A University, Busan 604-714, Republic of Korea
e-mail: jhlee@dau.ac.kr

lowest unoccupied molecular orbital (LUMO) energy levels, higher hole mobility, and significantly improved photovoltaic performance when compared to their corresponding alkoxy-substituted counterparts. Recent reports have shown that BDT based semiconducting polymers displayed power conversion efficiency (PCE) more than 9 % in bulk heterojunction (BHJ) PSCs [11]. Though the contemporary outcome is fairly agreeable, it is still necessary to find ideal π-conjugated polymers combining high PCE with convenient processability in order to meet the requirements of commercialized applications of PSCs. Therefore, more elaborate and systematic investigations that could provide an understanding the relationship between the structure and properties of the BDT based polymers would be required for the further development of highly efficient PSCs. In this scenario new type of aromatic side chains should be investigated to develop potential donor materials for extremely effective semiconducting π-conjugated polymers.

In the current OPV research trend, an optical spacer has been introduced in the device structure to increase the photocurrent [12]. The optical spacer also called as hole blocking layer is inserted between the photoactive layer and the top electrode so that the maximum light intensity is redistributed to be within the active charge separating BHJ layer. Recently, titanium sub-oxide (TiO_x) has been used as optical spacer and/or hole blocking layer in organic electronic devices that improves the efficiency of organic photovoltaic (OPV) cells. Similarly, a thin TiO_x layer functions as an electron injection layer in polymer light-emitting diodes (PLEDs) [13] as an internal separation layer with selective charge transport in multilayer bipolar FETs, and as a critical component in the architecture of polymer-based tandem solar cells [14]. Another most interesting application of TiO_x is as an encapsulation layer for enhancing the lifetimes of organic electronic devices [13].

Therefore, in this manuscript, we introduced 5-alkylbenzothiophene as a new conjugate side chain on BDT unit to the central phenyl ring to lower the HOMO levels and to broaden the absorption profile of the related polymers. It is worth stating that by incorporating benzothiophene as side chain, the conjugation of the molecule can be further extended. In order to ensure better solubility for the PSCs, we attached the moderate ethylhexyl group on donor unit. Considering the good planarity of BDT unit, good solubility, extended conjugation and the promising photovoltaic properties of the donor–acceptor (D–A) polymers, in this work, we synthesized a new derivative of BDT by introducing 5-ethylhexylbenzothiophene as a conjugate side chain on BDT unit and used it as donor unit for D-A polymers. Here, we synthesized two BDT-based copolymers represented by **P1** and **P2**, with two different acceptor building blocks including [7,7′-(3,3-diethylhexyl-3,4-dihydro-2H-thieno[3,4-b][1,4] dioxepine-6,8-diyl)bis(4-bromobenzo[c][1, 2, 5]thiadiazole)] (BT derivative) and diketopyrrolopyrrole (DPP) to tune the absorption and molecular energy levels to meet the requirements of highly efficient conjugated polymer donor materials. Conjugated polymers that employ electron-deficient derivatives of DPP and BT based monomers in the main chain are frequently used in PSCs and have provided excellent PCE [15, 16]. A common feature of both BT and DPP-based conjugated polymers used for photovoltaic cells is the lowoptical band gap, typically in the range of 1.35–1.65 eV, that creates a broad spectral response up to 700–1,000 nm. These polymers were obtained via Pd(0)-catalyzed Stille coupling polymerization. The BHJ PSCs were fabricated using the conventional device structures: ITO/PEDOT:PSS/polymer:$PC_{71}BM$/(with or without)TiO_x/Al. The solution processible TiO_x layer was introduced as an inter layer between the BHJ layer and the top metal (Al) electrode.

2 Experimental

2.1 Materials

All chemicals and reagents were purchased from Sigma-Aldrich Chemical Co. Ltd, Lumtec, TCI, Alfa Aesar, and Solenne BV and were used without further purification. Moisture sensitive reactions were conducted in the presence of nitrogen (N_2) atmosphere. THF was distilled over sodium and benzophenone was used as an indicator.

*2.1.1 Synthesis of 4,8-Bis(5-ethylhexylbenzothiophen-2-yl)benzo[1,2-b;4,5-b']dithiophene (**2**)*

n-BuLi (2.5 M, 1.81 mL) was added dropwise to a solution of 5-ethylhexylbenzothiophene (1.12 g, 4.54 mmol) in THF (50 mL) at 0 °C under N_2 atmosphere. The temperature of reaction mixture was raised to 50 °C and stirred for 1.5 h. 4,8-Dihydrobenzo[1,2-b:4,5-b']dithiophene-4,8-dione (0.5 g, 2.27 mmol) was added directly to the reaction mixture at 50 °C, which was then stirred for 2 h at the same temperature. Subsequently, the reaction mixture was cooled to room temperature and tin(II) chloride dihydrate (4.5 g) in 15 % HCl (20 mL) was added and further stirred for 1.5 h, which was poured into ice water. The reaction mixture was extracted with diethyl ether, the resultant organic layer was dried over anhydrous $MgSO_4$ and evaporated the solvent to get crude compound as brown oil. The crude product was then purified by column chromatography on silica gel using hexane as an eluent to obtain yellow solid **2** (0.9 g, 60 %).^{1}H NMR (300 MHz, $CDCl_3$): δ (ppm) 0.96 (m, 12H), 1.47–1.29 (br, 16H), 1.66 (m, 2H),

2.78 (m, 4H), 7.21 (m, 2H), 7.51 (d, 2H), 7.64 (d, 6H), 7.82 (d, 2H). ^{13}C NMR (300 MHz, $CDCl_3$): δ (ppm) 11.12, 14.37, 23.23, 25.92, 29.15, 32.34, 40.02, 41.64, 121.92, 123.16, 124.22, 124.36, 124.45, 126.56, 128.12, 136.88, 137.74, 138.50, 139.12, 139.98, 140.02.

2.1.2 Synthesis of 2,6-Bis(trimethyltin)-4,8-bis (5-ethylhexylbenzothiophen-2-yl)benzo [1,2-b;4,5-b']dithiophene (*3*)

A solution of compound **2** (1.2 g, 1.76 mmol) in THF (30 mL) was placed in 50 mL flask, which was flushed with N_2 and the solution was cooled to −78 °C using dry ice/acetone. To the cooled solution, tert-BuLi (1.7 M in pentane, 2.04 mL) was added slowly and stirred for another 30 min at −78 °C and trimethyltin chloride (0.71 g, 3.5 mmol) was directly added as a solid. The solution was slowly warmed to room temperature and allowed to stir for overnight. Aqueous sodium carbonate (30 mL) was added slowly to the solution and extracted with methylene chloride (MC) (100 mL). The resultant organic layer was dried over anhydrous $MgSO_4$ and evaporated the solvent to get yellow residue. The residue was recrystallized from ethanol to obtain yellow solid **3** (1.1 g, 59 %). ^{1}H NMR (300 MHz, $CDCl_3$): δ (ppm) 0.38 (s, 18H), 0.96 (m, 12H), 1.47–1.29 (br, 16H), 1.66 (m, 2H), 2.78 (m, 4H), 7.21 (m, 2H), 7.51 (d, 2H), 7.64 (d, 6H), 7.82 (d, 2H). ^{13}C NMR (300 MHz, $CDCl_3$): δ (ppm) −8.34, 11.12, 14.37, 23.23, 25.92, 29.15, 32.34, 40.02, 41.64, 121.78, 122.54, 124.04, 124.36, 126.34, 131.84, 137.46, 137.82, 138.28, 140.06, 140.98, 143.24, 143.66.

2.1.3 Synthesis of Poly[4,8-bis(5-ethylhexyl benzothiophen-2-yl)benzo[1,2-b:4,5-b′]dithiophene-alt-[7,7′-(3,3-diethylhexyl-3,4-dihydro-2H-thieno[3,4-b][1,4]dioxepine-6,8-di-yl)bis (benzo[c][1,2,5] thiadiazole)] (*P1*)

Stille polymerization condition was used for the synthesis of **P1** and **P2**. The synthesis of **P1** is explained completely as an illustrative example for other polymer. The 2,6-bis(trimethyltin)-4,8-bis(5-(5-ethylhexyl)benzothiophen-2-yl)benzo[1,2-b;4,5-b']dithiophene **3** (0.5 mmol) and monomer **4** (0.5 mmol) were mixed in anhydrous CB (15 mL). The reaction mixture was purged with N_2 for 20 min. $Pd_2(dba)_3$ (2 mol%, 6.8 mg) and P(o-tolyl)$_3$ (16 mol%, 20 mg) were added and the mixture was purged again with N_2. Then the reaction mixture was heated and stirred at 120 °C for 48 h. The polymerization reaction mixture was slowly cooled to room temperature, precipitated into methanol (MeOH) and filtered. The obtained solid was purified by Soxhlet method using MeOH, hexane and acetone. The polymer was obtained from CF, which was evaporated and precipitated into MeOH. The polymer was filtered and dried under vacuum to obtain **P1** as black solid (210 mg, 51 %, M_n = 30,700, PDI = 1.90).^{1}H NMR (300 MHz, $CDCl_3$): δ (ppm) 8.45–9.02 (m, 4H), 7.32–7.56 (m, 6H), 6.95–7.12 (br, 4H), 3.60–4.15 (br, 4H), 0.75–2.02 (m, 64H); Anal. Calcd for $C_{77}H_{88}N_4O_2S_7$: C, 69.75; H, 6.69; N, 4.23. Found: C, 69.04; H, 6.22; N, 4.02.

2.1.4 Synthesis of Poly[4,8-bis(5-ethylhexyl benzothiophen-2-yl)benzo[1,2-b:4,5-b']dithiophene-alt-[3,6-di(thiophen-2-yl)pyrrolo[3,4-c]pyrrole-1,4(2H,5H)-dione] (*P2*)

P2 was synthesized using 2,6-bis(trimethyltin)-4,8-bis(5-(5-ethylhexyl)benzothiophen-2-yl)benzo[1,2-b;4,5-b']dithiophene **3** and compound **5** as monomers with a similar method to that of **P1**. **P2** was obtained as a purple solid (145 mg, 47 %, M_n = 28,347, PDI = 1.74). ^{1}H NMR (300 MHz, $CDCl_3$): δ (ppm) 8.57–9.02 (m, 4H), 7.30–7.60 (m, 2H), 6.85–7.15 (m, 8H), 3.48–3.73 (br, 4H), 2.75–3.25 (br, 4H), 0.73–2.1 (m, 60H); Anal. Calcd for $C_{88}H_{116}N_2O_2S_6$: C, 74.11; H, 8.20; N, 1.96. Found: C, 73.86; H, 8.02; N, 1.73.

2.2 Methods

^{1}H and ^{13}C NMR spectra were recorded on a Varian Mercury Plus300 MHz spectrometer in $CDCl_3$ using tetramethylsilane as the internal reference. The chemical shifts were reported in ppm relative to the singlet of $CDCl_3$ at 7.26 and 77 ppm for the ^{1}H and ^{13}C NMR, respectively. The UV–visible spectra were recorded on a JASCO V-570 spectrophotometer at room temperature. TGA was carried out on a Mettler Toledo TGA/SDTA 851e, under N_2 atmosphere at heating rate of 10 °C/min. Weight averaged molecular weight (M_w), number-average molecular weight (M_n) and polydispersity index (PDI) were determined against polystyrene as standard by gel permeation chromatography (GPC) using PL gel 5 μm MLXED-C column on an Agilent 1100 series liquid chromatography system with tetrahydrofuran (THF) as an eluent. Cyclic voltammetry (CV) studies were carried out in a 0.1 M solution of tetrabutylammonium tetrafluoroborate in anhydrous acetonitrile at a scan rate of 100 mV/s using CHI 600C potentiostat (CH Instruments). A three electrode cell with platinum electrode as the working electrode, Ag/AgCl solution as the reference electrode and a platinum (Pt) wire as the counter electrode were used. Thin polymer films were coated on Pt electrode and dried before the experiment. The ITO-coated glass substrates were ultrasonically cleaned in detergent, water, acetone, and isopropyl alcohol. Then, a 40 nm thick layer of PEDOT:PSS (CLEVIOS^{TM}

AI 4083) was spin coated on the substrate. The coated buffer layer was cured at a temperature of 140 °C for 10 min in the air. The polymer:$PC_{71}BM$ was spin coated using a mixture of **P1/P2**:$PC_{71}BM$ (8:12 mg) that was dissolved in 1 mL of CB and further mixed with 1 vol% 1,8-diiodooctane (DIO) for **P1** and 2 vol% DIO for **P2** for optimized device performance. The TiO_x solution was spin cast in air on top of polymer:fullerene composite layer with a thickness around 10 nm. A 100 nm thick Al cathode with a defined area of 9 mm^2 was deposited via evaporation on the active layer. The thickness of the thin films was measured using a KLA Tencor Alpha-step IQ surface profilometer with an accuracy of ±1 nm. The performance of PSCs was measured using a calibrated AM1.5G solar simulator (Oriel® Sol3A™ Class AAA solar simulator, models 94043A) with a light intensity of 100 mW/cm^2 adjusted using a standard PV reference cell (2 × 2 cm^2, mono crystalline silicon solar cell, calibrated at NREL, Colorado, USA) and a computer controlled Keithley 2400 source measure unit. Incident photon to current conversion efficiency (IPCE) spectrum was measured using Oriel® IQE-200™. While measuring the J–V curves for PSC, a black mask was used and only the effective area of the cell was exposed to light irradiation. AFM images were acquired with a XE-100 (park system corp.) in tapping mode.

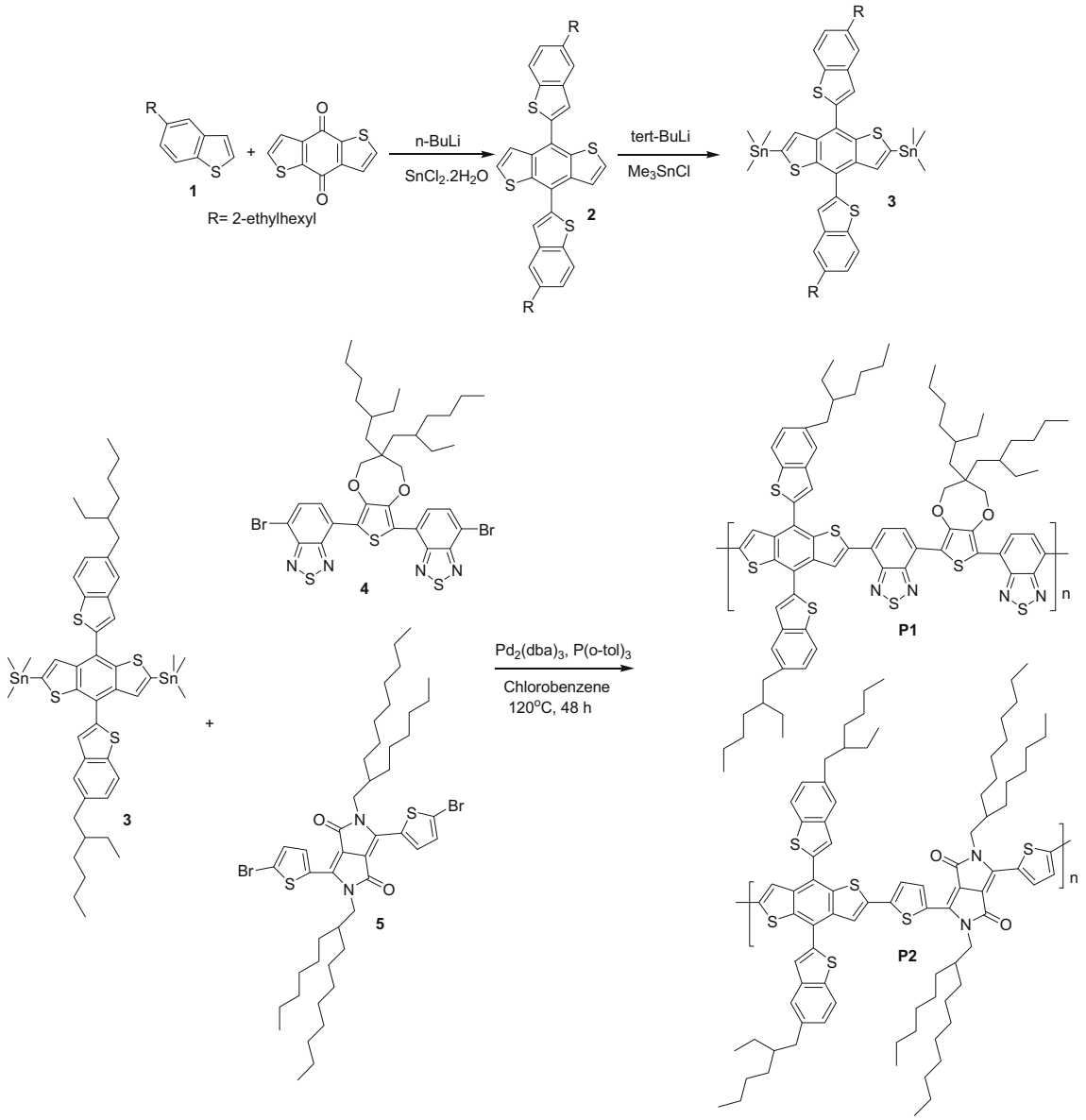

Scheme 1 Synthetic scheme of monomers and polymers

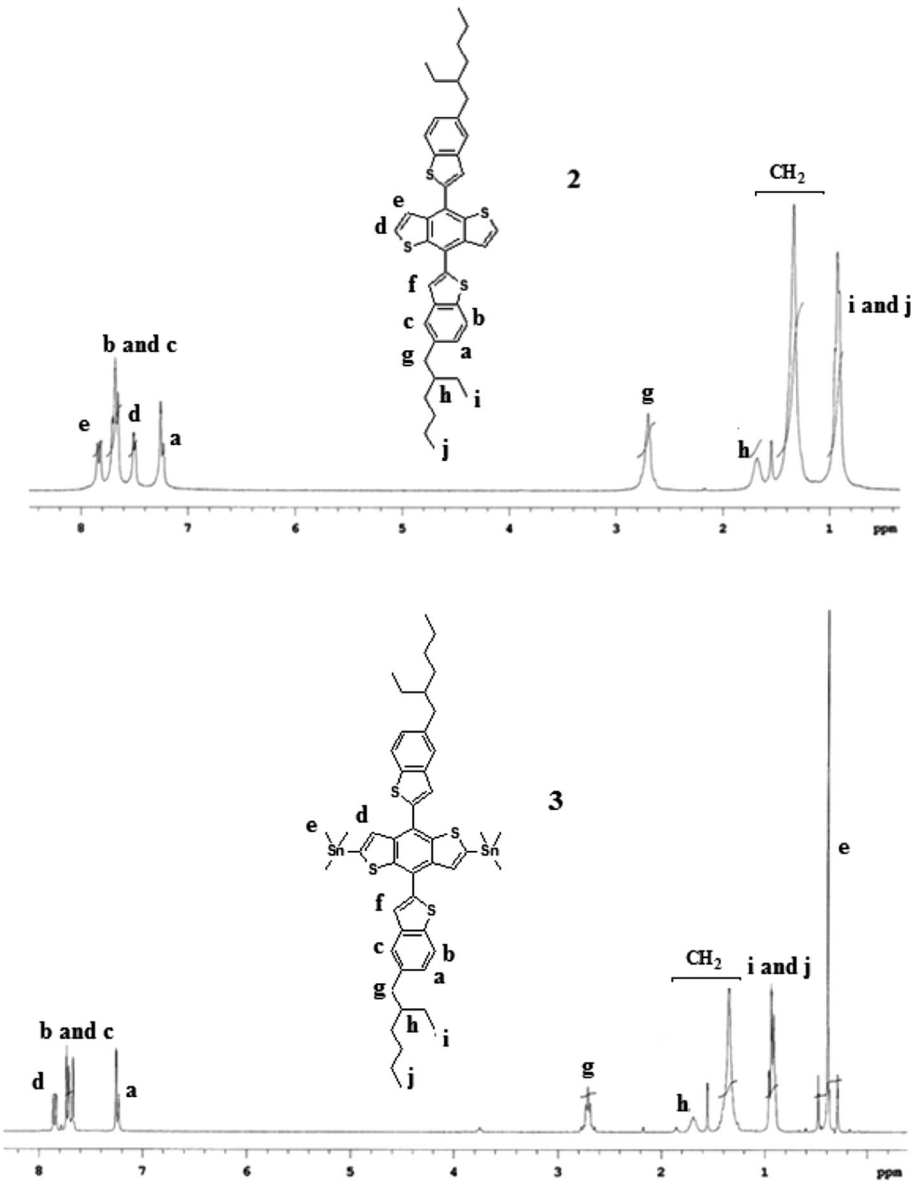

Fig. 1 ^{1}H NMR spectra of **2** and **3**

3 Results and Discussion

3.1 Synthesis and Characterization

The synthetic routes of new monomer and two polymers were depicted in Scheme 1. Synthesis of 5-ethylhexylbenzothiophene [17], 3,3′-diethylhexyl-3,4-propylenedioxythienyl-bisbenzothiadiazole [9], and TiO_x precursor solution [18] were followed according to similar procedure in the literature. Here, the synthesis of new BDT derivative with 5-ethylhexylbenzothiophene flanking as a side chain was illustrated. In order to ensure good solubility and high molecular weight of polymers, ethylhexyl was introduced at 5th position of benzothiophene. *n*-BuLi was added to 5-ethylhexylbenzothiophene to generate lithiated adduct. The reaction between 4,8-dihydrobenzo[1,2-b:4,5-b']dithiophene-4,8-dioneand lithiated 5-ethylhexylbenothiophene afforded the required compound **2**. Compound **2** was efficiently converted to the required distannylated monomer **3** using tert-BuLi and trimethyl tin chloride under N_2 atmosphere conditions with reasonable yield of 59 %. Accordingly, two D–A type polymers **P1** and **P2** were synthesized via typical Stille polymerization conditions. All polymerization reactions were conducted in presence of N_2 atmosphere using $Pd_2(dba)_3$ as a catalyst and P(o-tolyl)$_3$ as a corresponding ligand. The obtained polymers were readily soluble in organic solvents like chloroform (CF), THF, *o*-dichlorobenzene (ODCB), and chlorobenzene (CB). The monomer and polymers were characterized by ^{1}H and ^{13}C NMR spectroscopy (Figs. 1, 2, and 3).

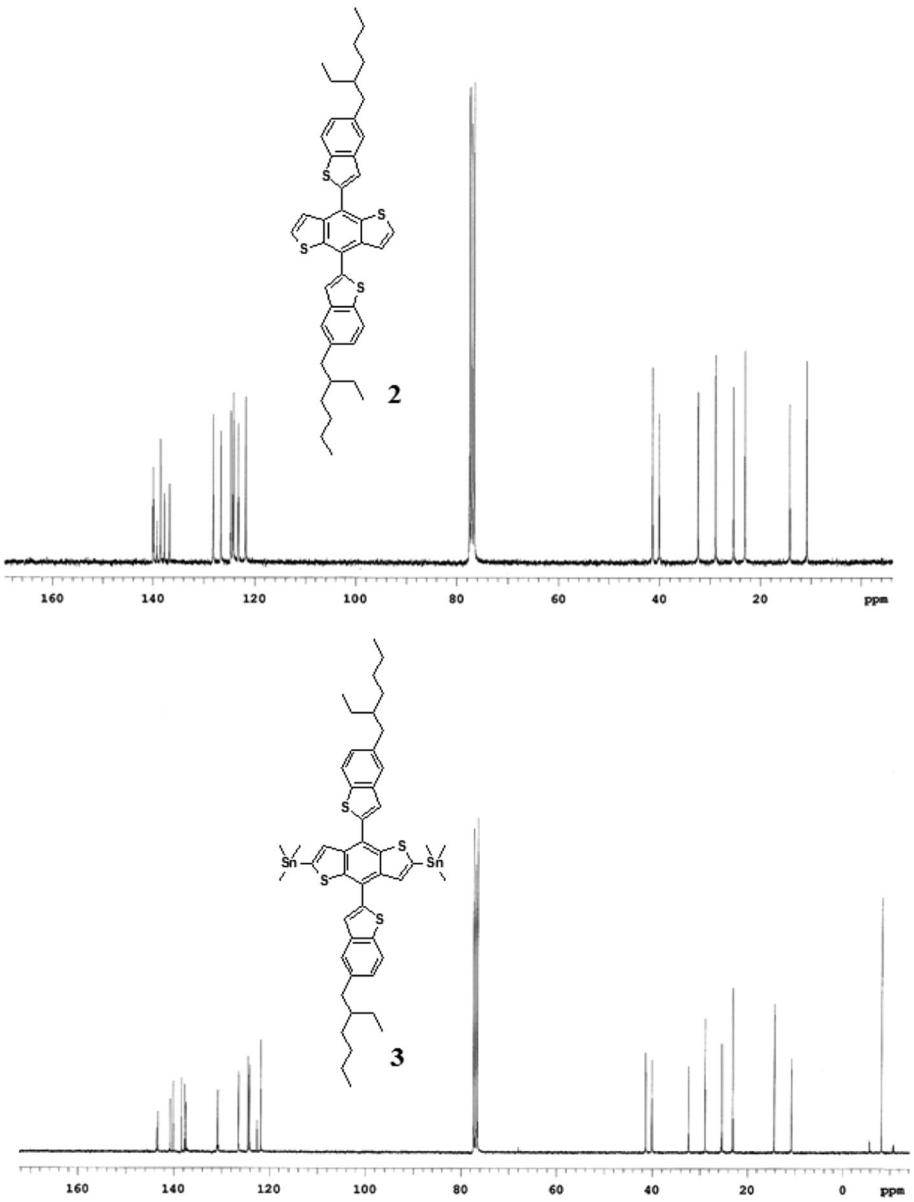

Fig. 2 ^{13}C NMR spectra of **2** and **3**

3.2 Thermal and Optical Properties

Thermal stability of the two polymers was investigated by using thermogravimetric analysis (TGA). As shown in Fig. 4, all these copolymers show good thermal stability under N_2 atmosphere with 5 % weight-loss temperatures (T_d) of 417 and 405 °C for **P1** and **P2**, respectively indicating good thermal stability for PSC applications. The introduction of alkylbenzothiophene side chains significantly improved the thermal stability of the BDT-based polymers, which is consistent with previous reports [19]. The normalized UV–visible absorption spectra of **P1** and **P2** in dilute CF solution and in thin films cast from CF are shown in Fig. 5, with the values of absorption maxima and edges listed in Table 1. The absorption maximum of **P1** in solution and film state were observed at 611 and 627 nm, where as the absorption maximum of **P2** in solution and film stae were located at 762 and 762 nm, respectively. The absorption maxium of **P1** and **P2** in solution were observed at 611 and 761 nm, respectively, whereas those of thin films were observed at 628, and 761 nm. The absorption spectra of the **P1** was slightly red-shifted (~17 nm) in the thin film due to the increased π–π interchain interactions upon aggregation. The optical bandgaps (E_g^{opt}) of **P1** and **P2** were calculated from an extrapolation of the absorption edges in the thin film states and were found to be 1.64 and 1.37 eV. It is noteworthy stating that the bandgap of **P2** is less compared to that of alkoxy or alkyl substituted BDT-based polymers [20]. The relatively low absorptivity in the visible region and high absorptivity in the near infrared

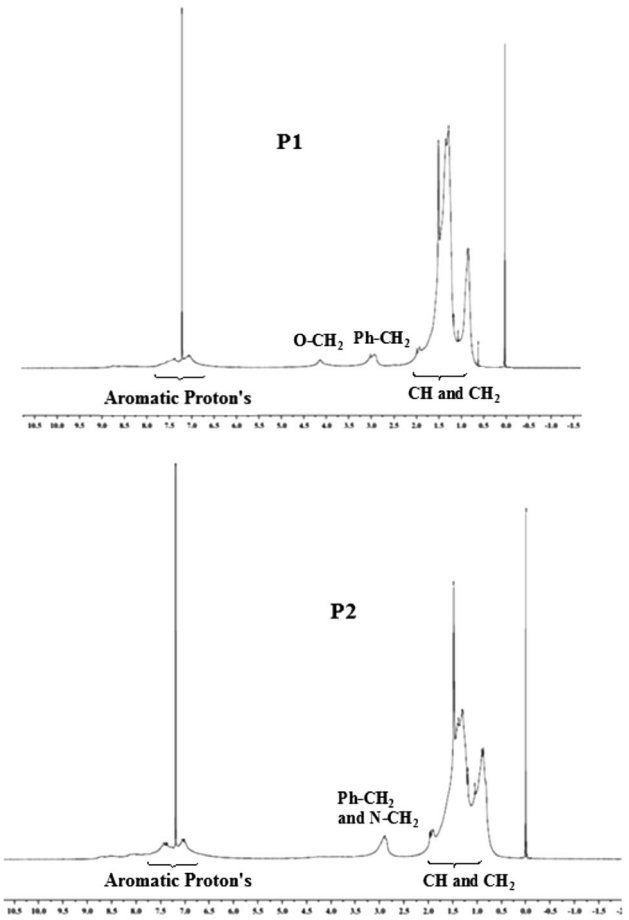

Fig. 3 ^{1}H NMR spectra of **P1** and **P2**

region of **P2** makes it a potential candidate for high performance tandem solar cells. The smaller bandgap and broad absorption of the new polymers should be beneficial to the application as photovoltaic material in PSCs.

3.3 Electrochemical Properties

The electrochemical properties of **P1** and **P2** were investigated using CV, which is shown in Fig. 6. The onset oxidation potentials of **P1** and **P2** were observed at 0.85 and 0.89 V, respectively. The HOMO energy levels of **P1** and **P2** were calculated to be −5.20 and −5.26 eV from their onset oxidation potential observed in CV. For good air stability, the HOMO energy level should have low value below air oxidation threshold limit (−5.2 eV) [21]. The HOMO energy levels of the **P1** and **P2** lie within the threshold limit, and the values denote that they possess good air stability and assure reasonable V_{oc}. The lower HOMO energy levels observed for **P1** and **P2** were attributed to the weak donating nature of 5-ethylhexylbenzothiophene, which is tethered perpendicularly on both sides of the phenyl ring in BDT core. The LUMO

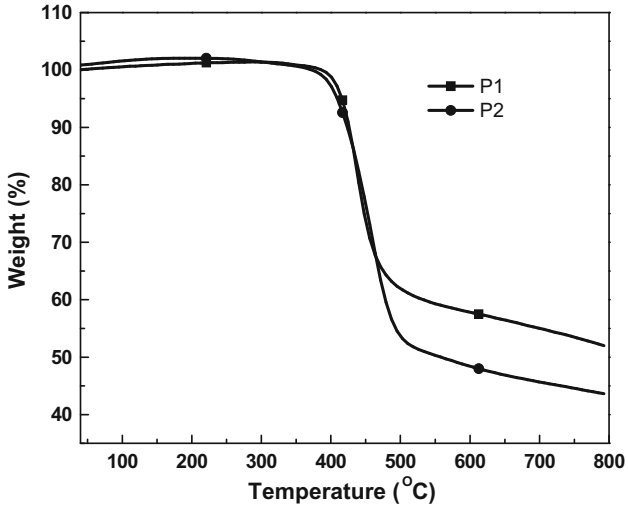

Fig. 4 TGA *curves* of **P1** and **P2**

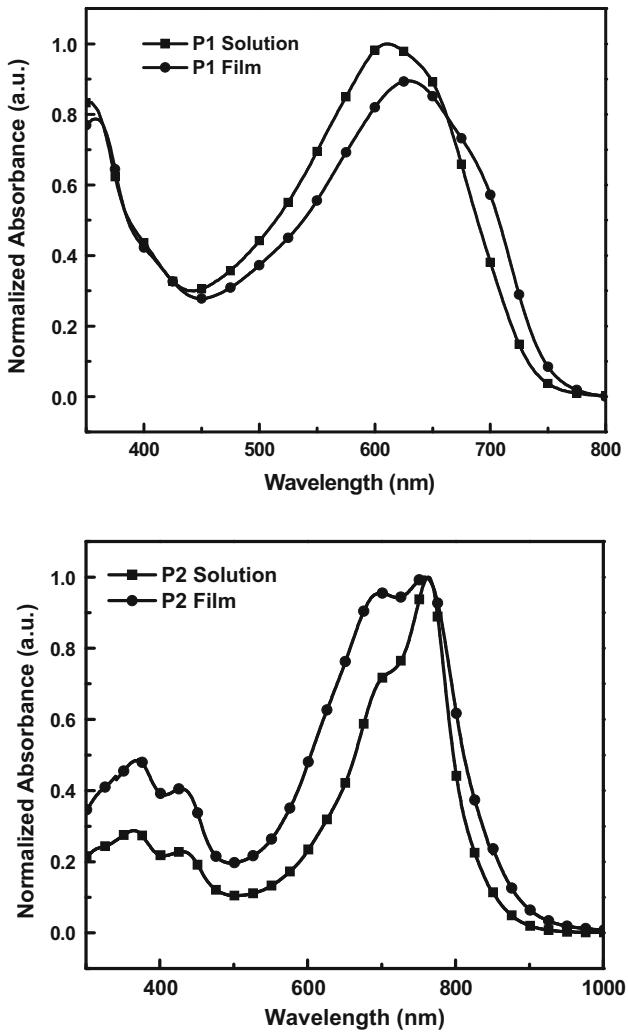

Fig. 5 Normalized UV–visible absorption spectra of **P1** and **P2** in CF solution and thin film state

Table 1 Optical and electrochemical properties of **P1** and **P2**

Polymer	Solution[a] λ_{max} (nm)	Film[b] λ_{max} (nm)	Film[c] λ_{max} (nm)	E_g^{opt} [d] (eV)	HOMO (eV)	LUMO (eV)
P1	611	627	756	1.64	−5.20	−3.56
P2	762	762	905	1.37	−5.26	−3.89

[a] Absorption maxima measured from UV–visible absorption spectrum in CF solution

[b] Absorption maxima measured from UV–visible absorption spectrum in thin film state

[c] The onset of the film absorption edge

[d] Estimated from the onset of the absorption in thin films ($E_g^{opt} = 1{,}240/\lambda_{onset}$)

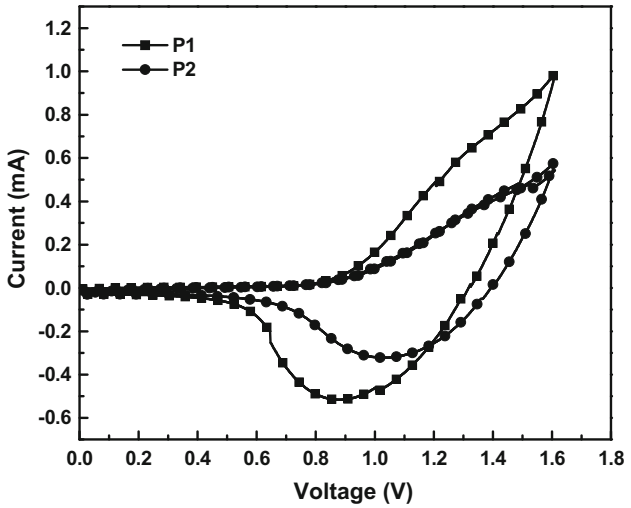

Fig. 6 Cyclic voltammogram of **P1** and **P2** in thin film state at a scan rate of 100 mV/s

energy levels were calculated from E_g^{opt} and HOMO energy levels obtained from CV [22] and were found to be −3.56 and −3.89 eV, respectively. The energy gap between LUMO energy level of the donor polymer and fullerene acceptor (greater than 0.3 eV) is a crucial factor in deciding the efficient exciton dissociation [23]. The LUMO energy levels of **P1** and **P2** are situated within the ideal range i.e., the energy levels lie higher than that of $PC_{71}BM$ (ca. −4.3 eV) [24]. The deep HOMO levels may have contributed to the improved oxidative stability and higher V_{oc}.

3.4 Photovoltaic and Morphological Characteristics

BHJ PSCs were fabricated using conventional device structure: ITO/PEDOT:PSS/polymer:$PC_{71}BM$/(with or without)TiO_x/Al and their photovoltaic performances were measured under 100 mW/cm^2 AM 1.5 G illumination. The optimized blend ratio was found to be 1:1.5 for both **P1** and

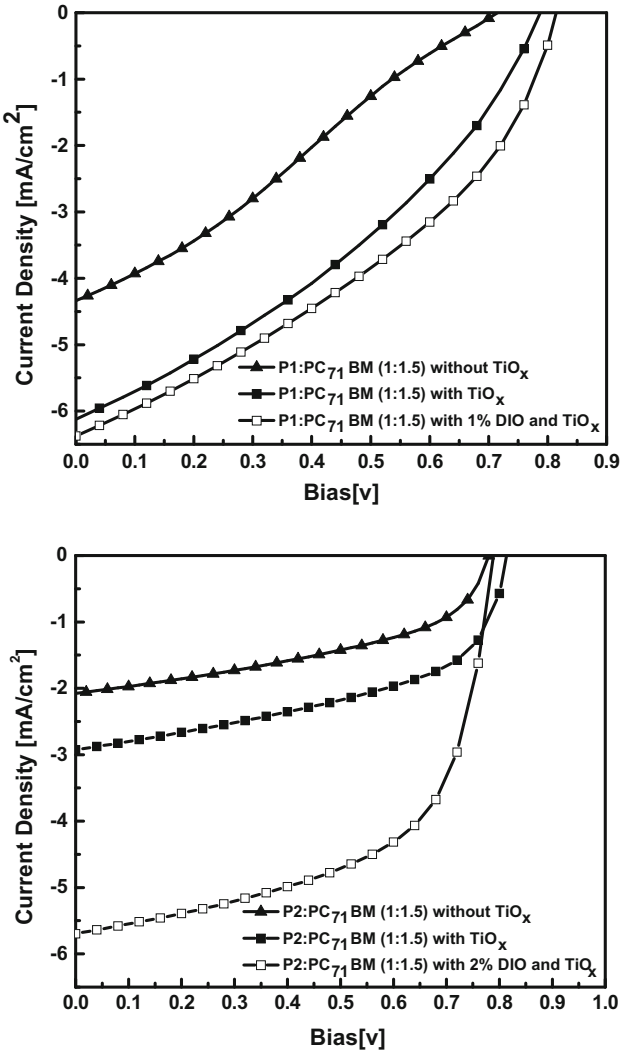

Fig. 7 Current density–voltage characteristics of BHJ PSCs based on polymer:$PC_{71}BM$ with and without DIO

P2. Figure 7 shows the current density–voltage (J–V) characteristics of the BHJ PSCs (with, without TiO_x and DIO) and the photovoltaic parameters V_{oc}, J_{sc}, FF, and PCE of the devices are summarized in Tables 2, 3 and 4. From our preliminary solvent screening, CB was preferred as the best solvent for our device studies and the polymer and $PC_{71}BM$ were mixed in CB. The solution processible TiO_x layer was introduced as an optical spacer and also as a hole blocker between the BHJ active layer and the top metal electrode. The TiO_x layer redistributes the light intensity within the BHJ by changing the optical interference between the incident light and the light reflected from the metal electrode. In order to improve the device performance, an optimal amount of the high boiling point additive DIO was added. The main idea behind the usage of additives is after adding a considerable amount of additive to the polymer:$PC_{71}BM$ blend, it can enhance the

Table 2 Photovoltaic characteristics of BHJ PSC devices without TiO_X

Polymer	Polymer:$PC_{71}BM$ (wt%)	J_{sc} (mA/cm^2)	Integrated J_{sc} (mA/cm^2)	V_{oc} (V)	FF (%)	PCE (%)
P1	1:1.5	4.33	4.15	0.72	27.31	0.85
P2	1:1.5	2.08	1.92	0.78	45.55	0.74

Table 3 Photovoltaic characteristics of BHJ PSC devices with TiO_X

Polymer	Polymer:PC_{71}BM (wt%)	J_{sc} (mA/cm^2)	Integrated J_{sc} (mA/cm^2)	V_{oc} (V)	FF (%)	PCE (%)
P1	1:1.5	6.12	6.11	0.78	34.87	1.68
P1[a]	1:1.5	6.45	6.27	0.81	36.88	1.93
P2	1:1.5	2.92	2.61	0.81	50.17	1.19
P2[b]	1:1.5	5.69	5.15	0.78	58.09	2.60

[a] 1 vol% DIO was used

[b] 2 vol% DIO was used

Table 4 Photovoltaic characteristics of BHJ PSC devices with different ratios

Polymer	Polymer:$PC_{71}BM$ (wt%)	J_{sc} (mA/cm^2)	V_{oc} (V)	FF (%)	PCE (%)
P1	1:1	5.43	0.79	29.93	1.29
P1	1:2	5.89	0.78	32.52	1.51
P2	1:1	2.15	0.82	46.85	0.83
P2	1:2	2.68	0.80	48.29	1.05

performance of the devices by forming better interpenetrating network in the BHJ active layer. Also, the additive acts as a mediator to have a homogeneous mixing with $PC_{71}BM$, thus improving its mixing with the polymer. All devices with and without TiO_x layer are fabricated using the same conditions to investigate the efficacy of TiO*x* on the BHJ film. When the PSC devices were fabricated without TiO_x layer, a maximum PCE of 0.85 and 0.74 % was measured for **P1**:$PC_{71}BM$ (1:1.5 wt%) and **P2**:PC_{71}BM (1:1.5 wt%) system, respectively (the results are summarized in Table 2). After introducing TiO_x layer between the Al cathode and active layer, the PSC devices show an increment in the PCE when compared to the devices without TiO_x layer. A maximum PCE of 1.68 and 1.19 % and J_{sc} of 6.12 and 2.92 mA/cm^2 were realized, when pristine CB was used as a solvent for **P1**:$PC_{71}BM$ (1:1.5 wt%) and **P2**:$PC_{71}BM$ (1:1.5 wt%) system (the results are summarized in Tables 3 and 4). The measured V_{oc} of the **P1** and **P2** lies between 0.78 and 0.81 V, which is in agreement with the theoretically predicted values calculated from the HOMO of the donor polymer and LUMO of fullerene derivative ($PC_{71}BM$) [19]. The V_{oc} of PSCs based on **P2** were measured as 0.81 V, while the reported value for the corresponding alkoxy substituted BDT was 0.66 V. This can be explained by the fact that the HOMO level is increased by replacing the alkoxy group with the alkylbenzothiophene group. The larger decrease of J_{sc} witnessed for **P2** is likely due to the unfavorable morphology of the photo active layer. The higher FF obtained for **P2** is most likely due to the good ohmic contacts between the interlayers that had formed during the device fabrication.

To further increase the photovoltaic performance of **P1** and **P2**, DIO was used as an additive as previously reported by other research groups [25]. It is very important to achieve excellent interpenetrating nanoscale morphology to get high J_{sc}, which has direct impact on deciding the photovoltaic performance of BHJ PSCs. In similar to previous reports, the PCE of both polymers **P1** and **P2** increased upon the addition of DIO [26]. Clearly, a considerable enhancement of J_{sc} and FF is also predicted and is proved by J_{sc} values provided in Table 2. In particular, **P2** exhibit a great increment in FF (from 50.17 to 58.09 %) and J_{sc} (from 2.92 to 5.69 mA/cm^2) when 2 vol% DIO was used as a processing additive. The superior FF is probably due to the effective and improved intermolecular packing assisted by the alkylbenzothiophene side chain substituent. Thus, an increased PCE of 1.93 and 2.60 % with 1 and 2 % DIO were achieved for the devices based on **P1** and **P2**, respectively. It is worth noting that the device **P2-**based device, which is a combination of alkylbenzothiophene substituted BDT and DPP based acceptor stood as a champion device with PCE of 2.60 %. Figure 8 shows the external quantum efficiency (EQE) curves of the devices based on **P1**:$PC_{71}BM$ and **P2**:$PC_{71}BM$ without additive and with DIO. These devices exhibited broad EQE

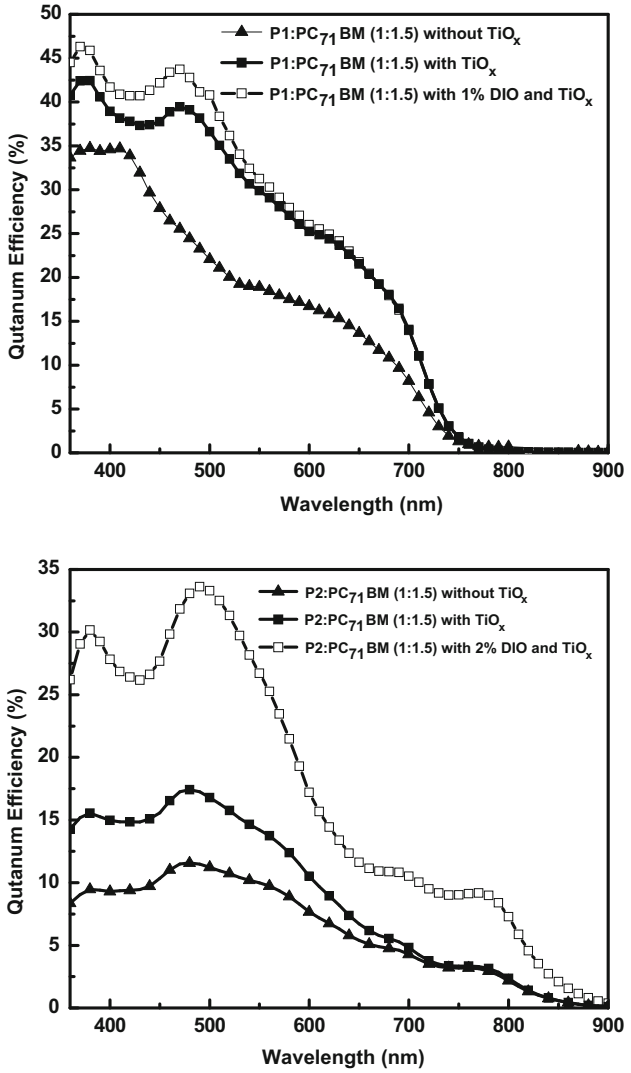

Fig. 8 EQE *curves* of the BHJ PSCs based on polymer:$PC_{71}BM$ with and without DIO

responses with maximum IPCE values of 44 % at 467 nm and 33 % at 490 nm for the PSCs based on **P1** and **P2** (with DIO), respectively. The IPCE results are consistent with the J_{sc} values of the corresponding PSCs.

The surface morphology of the active layer of BHJ PSCs was investigated by atomic force microscopy (AFM). The enhancement in the OPV performances was caused by the changes in the morphology of the blend film. The morphological requirement for the active layer in high performance PSCs is nanoscale phase separation, better continuous percolating path for hole and electron transport to the corresponding electrodes. Figure 9 shows the AFM images and height profiles of the blend films with and with out DIO. The measured root mean square (RMS) roughness of the pristine active layers was 1.03 nm for P1 and 0.62 nm for P2. In general, nanoscale phase separation has

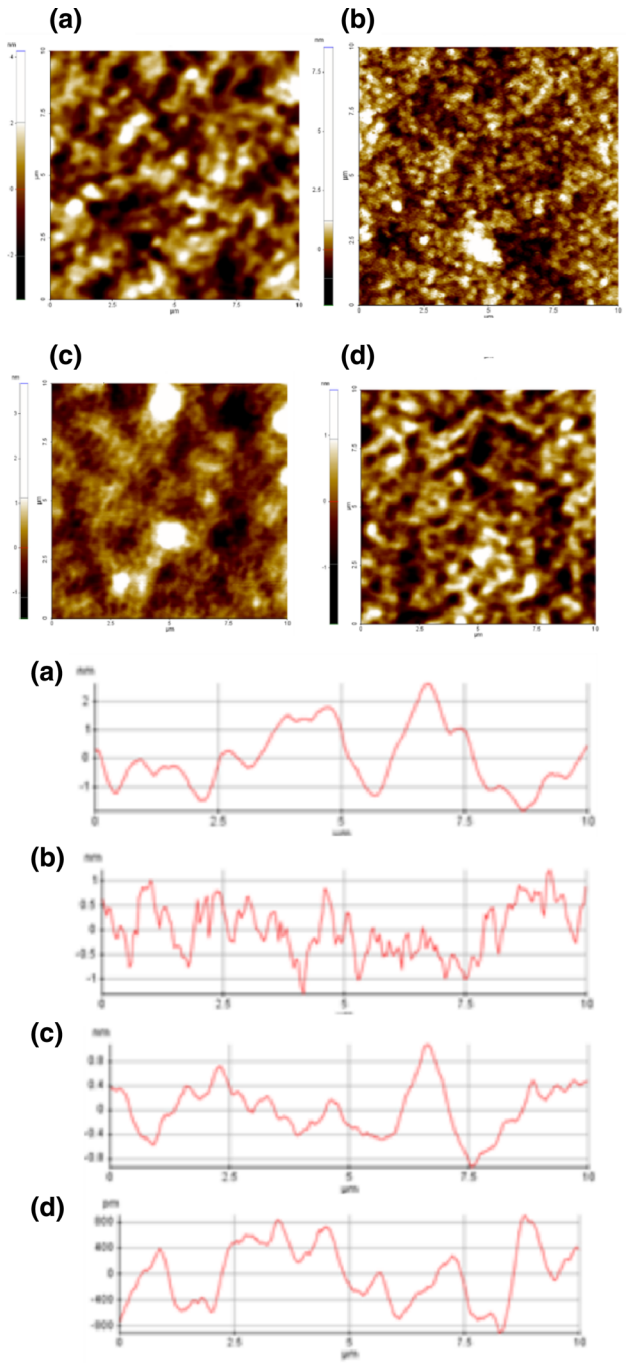

Fig. 9 AFM images and height profiles of the BHJ PSCs based on **a P1**:$PC_{71}BM$ **b P1**:$PC_{71}BM$ with 1 % DIO **c P2**:$PC_{71}BM$ **d P2**:PC_{71} BM with 2 % DIO

to be established to allow efficient charge separation due to the short exciton diffusion length (10 mm) of the donor polymers. AFM images clearly showed that there were large domains in the blend film prepared using only CB; these large domains would diminish exciton migration to the donor/acceptor interface and are not favorable for charge separation. The measured RMS roughness of the

active layers was after introducing DIO was 0.62 nm for P1 and 0.48 nm for P2. The surface roughness of the polymer:$PC_{71}BM$ blends decreased, when optimal amount of DIO was added to the CB solution [27]. Accordingly, the PCE of the PSC devices were enhanced upon introducing DIO. The morphology of the blend films prepared using the CB/DIO mixed solvent wasmuch more uniform, with no significant phase separation. Better miscibility between the donor polymer and the $PC_{71}BM$ was formed thus providing excellent interpenetrating networks for charge transport; these factors may have led to increase in the J_{sc} value.

4 Conclusions

A new BDT monomer with 5-ethylhexylbenzothiophene substituent has been synthesized. Stille coupling of the new BDT unit with 3,3′-diethylhexyl-3,4-propylenedioxythienyl-BBT and 3,6-di(thiophen-2-yl)pyrrolo[3,4-c]pyrrole-1,4(2H,5H)-dione (DPP) produced two D–A polymers **P1** and **P2**, respectively. Introduction of 5-alkylbenzothiophene on BDT unit leads to better solubility and deeper HOMO energy levels (ca. −5.2 eV) of the copolymers, and the different electron deficient units regulate the bandgap of the D–A polymers from 1.64 eV for **P1** to 1.37 eV for **P2**. The photovoltaic results of **P1** and **P2** shows that the devices with TiO_x layer exhibits an enhancement of PCE, as compared to the corresponding conventional devices without the TiO_x spacer. Both polymers showed good photovoltaic performances: **P1** with a PCE of 1.93 % and **P2** with a PCE of 2.60 %. Though the photovoltaic performance of the polymers is quite low, the results indicate that the D–A polymers based on the alkylbenzothiophene substituted BDT donor unit will allows additional structural tuning to produce highly efficient π-conjugated polymers for use in solar cells.

Acknowledgments This work was supported by Grant fund from the National Research Foundation (NRF) (2011-0028320) and the Pioneer Research Center Program through the NRF (2013M3C1A3065522) by the Ministry of Science, ICT & Future Planning (MSIP) of Korea. JHL acknowledges a financial support by Basic Science Research Program through the National Research Foundation of Korea (NRF) funded by the Ministry of Education, Science and Technology (2012-0531).

References

1. H. Pan, Y. Li, Y. Wu, P. Liu, B.S. Ong, S. Zhu, G. Xu, Chem. Mater. **18**, 3237–3241 (2006)
2. Y. Liang, D. Feng, Y. Wu, S.-T. Tsai, G. Li, C. Ryu, L. Yu, J. Am. Chem. Soc. **131**, 7792–7799 (2009)
3. P. Sista, M.P. Bhatt, A.R. McCary, H. Nguyen, J. Hao, M.C. Beiwer, M.C. Stefan, J. Polym. Sci. A **49**, 2292–2302 (2011)
4. P. Sista, J. Hao, S. Elkassih, E.E. Sheina, M.C. Beiwer, B.G. Janesko, M.C. Stefan, J. Polym. Sci. A **49**, 4172–4179 (2011)
5. Y. He, Y. Zhou, G. Zhao, J. Min, X. Guo, B. Zhang, M. Zhang, J. Zhang, Y. Li, F. Zhang, O.J. Inganaes, J. Polym. Sci. A **48**, 1822–1829 (2010)
6. T.-Y. Chu, J.P. Lu, S. Beapuré, Y. Zhang, J.-R. Pouliot, J. Zhou, A. Najari, M. Leclerc, Y. Tao, Adv. Funct. Mater. **22**, 2345–2351 (2012)
7. C. Piliego, T.W. Holcombe, J.D. Douglas, C.H. Woo, P.M. Beaujuge, J.M. Frechet, J. Am. Chem. Soc. **132**, 7595–7597 (2010)
8. H.-Y. Chen, J. Hou, S. Zhang, Y. Liang, G. Yang, Y. Yang, L. Yu, Y. Wu, G. Li, Nat. Photonics **3**, 649–653 (2009)
9. N. Chakravarthi, K. Kranthiraja, M. Song, K. Gunasekar, P. Jeong, S.-J. Moon, I.-N. Kang, J.W. Lee, S.-H. Jin, Sol. Energy Mater. Sol. Cells **122**, 136–145 (2014)
10. L. Huo, S. Zhang, X. Guo, F. Xu, Y. Li, J. Hou, Angew. Chem. Int. Ed. **50**, 9697–9702 (2011)
11. S. Zhang, L. Ye, W. Zhao, D. Liu, H. Yao, J. Hou, Macromolecules **47**, 4653–4659 (2014)
12. K. Lee, J.Y. Kim, S.H. Park, S.H. Kim, S. Cho, A.J. Heeger, Adv. Mater. **19**, 2445–2449 (2007)
13. S.H. Kim, J.Y. Kim, S.H. Park, K. Lee, Proc. SPIE-Int. Soc. Opt. Eng. **5937**, 59371 G (2005)
14. J.Y. Kim, K. Lee, N.E. Coates, T.-Q. Nguyen, M. Dante, A.J. Heeger, Science **317**, 222–225 (2007)
15. L. Dou, J. Gao, E. Richard, J. You, C.-C. Chen, K.C. Cha, Y. He, G. Li, Y. Yang, J. Am. Chem. Soc. **134**, 10071–10079 (2012)
16. N. Wang, Z. Chen, W. Wei, Z. Jiang, J. Am. Chem. Soc. **135**, 17060–17068 (2013)
17. S. Bobinger, J. Anderson, Environ. Sci. Technol. **43**, 8119–8125 (2009)
18. S. Cho, K. Lee, A.J. Heeger, Adv. Mater. **21**, 1–4 (2009)
19. R. Duan, L. Ye, X. Guo, Y. Huang, P. Wang, S. Zhang, J. Zhang, L. Huo, J. Hou, Macromolecules **45**, 3032–3038 (2012)
20. Y. Wang, F. Yang, Y. Liu, R. Peng, S. Chen, Z. Ge, Macromolecules **46**, 1368–1375 (2013)
21. D.M. de Leeuw, M.M.J. Simenon, A.R. Brown, R.E.F. Einehand, Synth. Met. **87**, 53–59 (1997)
22. C.J. Brabec, C. Winder, N.S. Sariciftici, J.C. Hummelen, A. Dhanabalan, P.A. van Hal, R.A.J. Janssen, Adv. Funct. Mater. **12**, 709–712 (2002)
23. J.-L. Brédas, D. Beljonne, V. Coropceanu, J. Cornil, Chem. Rev. **104**, 4971–5004 (2004)
24. L. Zhang, K. Pei, M. Yu, Y. Huang, H. Zhao, M. Zeng, Y. Wang, J. Gao, J. Phys. Chem. C **116**, 26154–26161 (2012)
25. Y. Zhang, Z. Li, S. Walkim, S. Alem, S.-W. Tsang, J. Lu, J. Ding, Y. Tao, Org. Electron. **12**, 1211–1215 (2011)
26. X. Wang, P. Jiang, Y. Chen, H. Luo, Z. Zhang, H. Wang, X. Li, G. Yu, Y. Li, Macromolecules **46**, 4805–4812 (2013)
27. B.R. Aïch, J. Lu, S. Beaupré, M. Leclerc, Y. Tao, Org. Electron. **13**, 1736–1741 (2012)